

## Original Research

# Effects of Individual and Coexisting Diabetes and Cardiomyopathy on Diastolic Function in Rats (*Rattus norvegicus domestica*)

Pitipat Kitpipatkun,<sup>1</sup> Akira Yairo,<sup>1</sup> Konosuke Kato,<sup>1</sup> Katsuhiko Matsuura,<sup>1</sup> Danfu Ma,<sup>1</sup> Seijirow Goya,<sup>1</sup> Akiko Uemura,<sup>2</sup> Ken Takahashi,<sup>3</sup> and Ryo Tanaka<sup>1,\*</sup>

The goal of this study was to evaluate diastolic intraventricular pressure gradients (IVPG) and 2-dimensional tissue tracking (2DTT) patterns during diabetes and cardiomyopathy. Rats ( $n = 60$ ) were induced to become diabetic (DM group,  $n = 15$ ) by using streptozotocin, to become cardiomyopathic (CM group,  $n = 15$ ) by using isoproterenol, and to become both diabetic and cardiomyopathic (DMCM group,  $n = 15$ ); control rats (CT group,  $n = 15$ ) were injected with saline. Two months after induction, all rats underwent conventional echocardiography, IVPG, and 2DTT and then were euthanized for microscopic examination of cardiac fibrosis. Compared with the controls, all 3 treated groups showed diastolic dysfunction and delayed cardiac relaxation. DMCM rats showed the most pronounced cardiac abnormalities. In addition, CM and DMCM groups had showed decreased middle IVPG, whereas DMCM rats had decreased midapical IVPG. Although the overall IVPG of the CM group was normal, the middle segment was significantly decreased. 2DTT results showed that the DMCM group had a delay in relaxation compared with other groups. IVPG and 2DTT can be used to overcome the limitation of conventional echocardiographic methods and reveal diastolic dysfunction. DM worsened diastolic function during cardiac disease.

**Abbreviations:** 2DTT, two-dimensional tissue tracking; DM, diabetes mellitus; HR, heart rate; IVPD, intraventricular pressure difference; IVPG, intraventricular pressure gradient; LV, left ventricle; LVM, left ventricular mass; MTC, Masson trichrome

DOI: 10.30802/AALAS-CM-20-000042

Diabetes mellitus (DM) is a chronic disease identified by hyperglycemia.<sup>1</sup> DM and associated insulin abnormalities result in hypertension, cardiovascular disease, and multiple organ dysfunction.<sup>18</sup> Diabetic cardiomyopathy is defined as abnormal myocardial structure and performance in the absence of other cardiac risk factors, such as coronary artery disease, hypertension, and significant valvular disease, in patients with DM.<sup>3</sup> A previous study showed that diastolic dysfunction could result from DM; and cardiac fibrosis in the interstitial and perivascular areas was a hallmark of long-term DM.<sup>23</sup> Cardiac fibrosis in DM rats results from myocardial infarction.

Cardiomyopathy can be induced in rats by using isoproterenol.<sup>17</sup> Cardiomyopathy refers to the cardiac disorder in which myocardial abnormalities result from myocyte injury. Cardiomyopathy has several etiologies, including chronic hypertension, valvular abnormality, and toxin.<sup>15</sup> Both DM and cardiomyopathy are fibrotic heart diseases, but their pathogenesis differs. Moreover, DM and CM cause fibrosis in different heart locations.

The diastolic function of the left ventricle (LV) can be defined as the pull of blood into the LV under low filling pressure. Two groups have described the pressure differences that pull the blood through the mitral valve into the ventricle during diastole.<sup>6,16</sup> The difference of pressure between the LV and aorta during systole and the importance of regional pressure differences within the ventricle during relaxation has recently gained attention.<sup>9,29</sup> The diastolic intraventricular pressure gradient (IVPG) in the LV is closely related to LV relaxation. Deterioration of the IVPG is associated with abnormal LV blood flow patterns.<sup>2</sup>

2D tissue tracking (2DTT) echocardiography is a promising technique that quantifies myocardial deformation by tracking the ultrasonographic speckle pattern of the cardiac cycle.<sup>13</sup> Because of the importance of measuring diastolic function, we used conventional echocardiography, IVPG and 2DTT to evaluate the diastolic impairment without altering systolic function. We studied the relationship between mild (DM rats) and moderate (CM rats) cardiac fibrosis due to myocardial injury and infarction together with the severe fibrosis that develops due to the combination of DM and cardiomyopathy.

Streptozotocin and isoproterenol were used to induce DM and cardiomyopathy, respectively. Both cause cardiac fibrosis, but the pathogenesis and affected location are different. Our study was designed to evaluate diastolic IVPG and 2DTT as diastolic indices. Our goal was to delineate IVPG and 2DTT patterns in DM, CM, and very severe fibrotic heart disease induced by combining DM and cardiomyopathy.

Received: 01 Jun 2020. Revision requested: 20 Jul 2020. Accepted: 30 Sep 2020.

<sup>1</sup>Department of Veterinary Surgery, Faculty of Veterinary Medicine, Tokyo University of Agriculture and Technology, Tokyo, Japan; <sup>2</sup>Department of Clinical Veterinary Medicine, Division of Veterinary Research, Obihiro University of Agriculture and Veterinary Medicine, Hokkaido, Japan; and <sup>3</sup>Department of Pediatrics and Adolescent Medicine, Faculty of Medicine, Juntendo University Graduate School of Medicine, Tokyo, Japan

\*Corresponding author. Email: ryo@vet.ne.jp

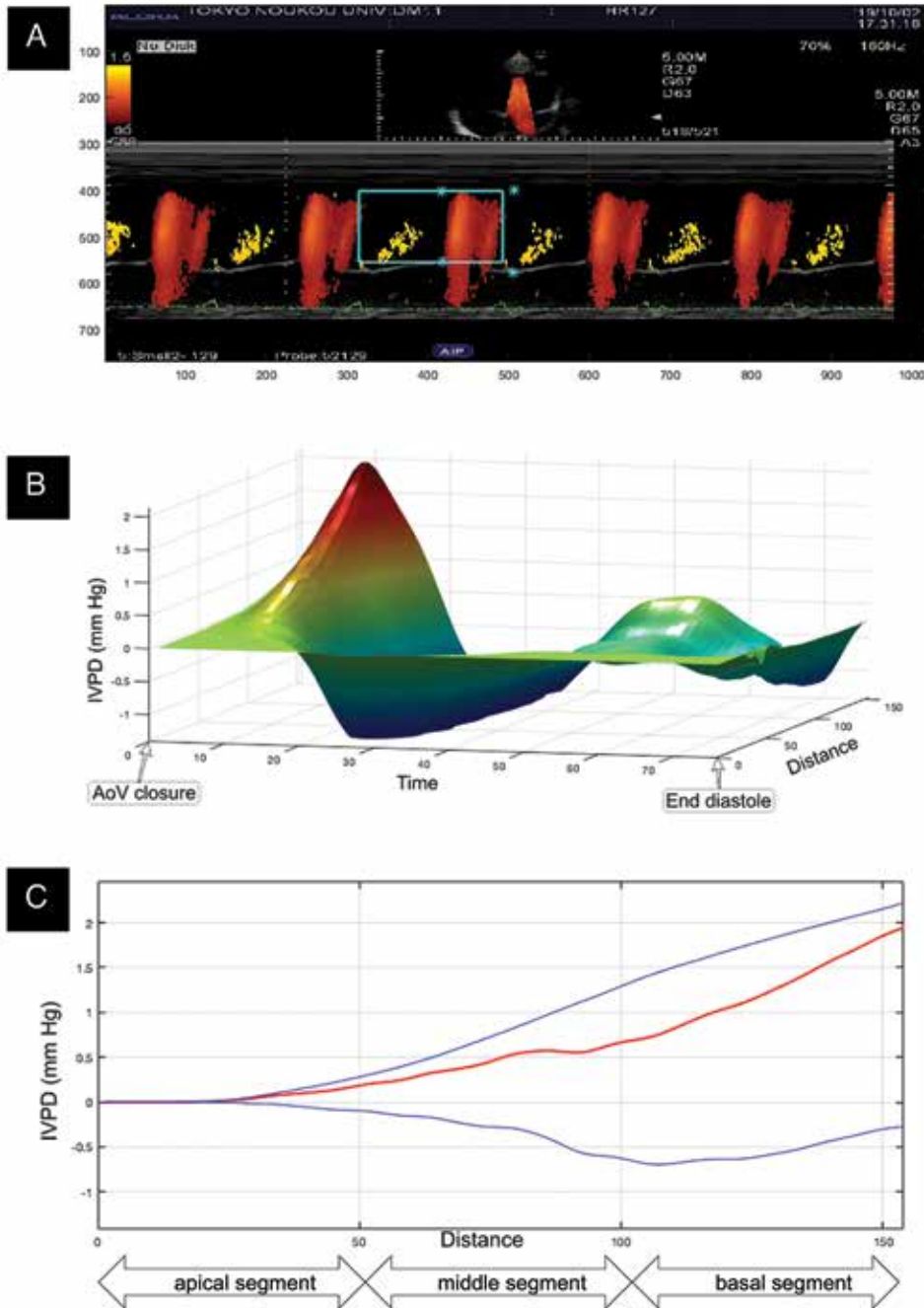


**Figure 1.** The mitral inflow patterns are colorized by using pulsed-wave Doppler along the flowing of the blood into the LV and captured during M-mode (A) The IVPD is calculated by the specific algorithm of MATLAB software, then the 3D (3D) temporal and spatial profile of the IVPD is generated (B) In 3D image, the x, y and z axes represent time, IVPD, and distance, respectively. Subsequently, the IVPD in early diastole are identified (C) The top (blue), middle (red), and bottom (blue) lines represent inertial, total, and convective IVPD, respectively; *AoV* aortic valve; IVPG = IVPD , distance (mm Hg/cm).

### Materials and Methods

**Animal preparation.** Healthy male Sprague–Dawley rats ( $n = 60$ ; weight, 250 to 350 g; age, 5 to 6 mo; Charles River Laboratories, Japan) were housed individually in plastic cages with wood bedding material (Aspen Bed I, American Excelsior Company, USA) and under controlled conditions of  $25 \pm 0.5$  °C and a 12:12-h light:dark cycle in a ventilated room and received tap water and a standard rat food (MF, Oriental Yeast, Japan) ad libitum.

Rats were divided into 4 groups. Rats in the DM group ( $n = 15$ ) received 60 mg/kg of streptozotocin (Wako Pure

Chemical Industries, Japan) as a single peritoneal injection to induce DM. At 2 wk after injection, Glucose PILOT (Aventir Biotech, Carlsbad, CA) was used according to the manufacturer’s guidance to measure the blood glucose level. The tip of the rat’s tail was stabbed and one drop of blood was used for measuring. Only rats whose glucose concentration was 350 mg/dL or greater were retained as study subjects of this group. Rats in the CM group ( $n = 15$ ) received daily intraperitoneal injections of 2.5 mg/kg of isoproterenol (Tokyo Chemical Industry, Japan) for 7 d to induce cardiomyopathy. Animals in the DMCM group ( $n = 15$ ) were treated with both streptozotocin

**Table 1.** The echocardiographic and other parameters prior (PRE) enrolling the experiment and post (POST) induction of the diseases for 2 mo.

Parameters	CT			DM			CM			DMCM		
	PRE	POST	<i>P</i>	PRE	POST	<i>P</i>	PRE	POST	<i>P</i>	PRE	POST	<i>P</i>
BW (g)	286 (262–320)	329 (309–342)	= 0.0026*	283 (267–309)	300 (268–315)	= 0.6455	304 (259–328)	336 (316–352)	= 0.0026*	297 (266–321)	253 (226–277)	= 0.0009*
BG (mg/dL)	127 (118–151)	137 (111–161)	= 0.9259	135 (116–164)	475 (442–501)	< 0.0001*	128 (87–158)	107 (92–140)	= 0.6610	131 (106–153)	473 (422–502)	< 0.0001*
LVIDd (mm)	7.5 (7.3–7.8)	8.0 (7.5–8.3)	= 0.0069	7.5 (7.3–7.8)	7.4 (6.7–7.6)	= 0.1199	7.9 (7.6–8.3)	8.8 (8.5–9.1)	< 0.0001*	7.8 (7.5–8.2)	7.8 (7.4–8.2)	= 0.6722
LVIDs (mm)	4.5 (4.0–4.7)	5.3 (4.8–5.4)	= 0.0004*	4.6 (4.2–4.7)	4.4 (4.3–4.8)	= 0.7654	4.8 (4.5–5.1)	5.8 (5.5–6.1)	= 0.0001*	4.9 (4.2–5.2)	4.9 (3.4–5.3)	= 0.7351
LVPWd (mm)	1.8 (1.6–2.0)	1.6 (1.6–1.8)	= 0.0595	1.6 (1.4–1.8)	1.4 (1.2–1.6)	= 0.0336*	1.8 (1.6–1.9)	2.0 (1.9–2.1)	= 0.0051*	1.7 (1.6–1.9)	1.4 (1.3–1.5)	= 0.0065*
LVPWs (mm)	2.6 (2.4–2.8)	2.2 (2.2–2.4)	= 0.0079*	2.7 (2.4–2.9)	2.5 (2.0–2.5)	= 0.0063*	2.6 (2.3–2.7)	2.8 (2.7–2.9)	= 0.0024*	2.5 (2.4–2.6)	2.8 (2.0–3.1)	= 0.4045
LVM (mg)	757 (683–845)	757 (693–775)	= 0.4420	712 (626–759)	518 (463–544)	= 0.0002*	742 (685–790)	1075 (945–1117)	< 0.0001*	697 (640–741)	640 (532–741)	= 0.1084
HR (bpm)	353 (348–356)	320 (293–323)	< 0.0001*	335 (320–347)	270 (251–275)	< 0.0001*	330 (319–345)	290 (283–300)	= 0.0002*	328 (299–342)	222 (214–231)	< 0.0001*
E (cm/s)	121 (118–126)	111 (107–120)	= 0.0041*	114 (110–120)	77 (74–82)	< 0.0001*	118 (115–120)	89 (74–98)	< 0.0001*	118 (111–123)	74 (59–76)	< 0.0001*
A (cm/s)	FU	FU		FU	PF		FU	FU, PF, SP		FU	SP	
Septal <i>s'</i> (cm/s)	4.1 (3.9–5.0)	3.5 (2.9–6.3)	= 0.0649	4.3 (3.8–4.6)	2.9 (2.7–3.2)	< 0.0001*	4.2 (3.4–4.4)	3.6 (2.9–3.9)	= 0.3187	3.8 (3.7–5.0)	2.1 (1.8–2.5)	< 0.0001*
Septal <i>e'</i> (cm/s)	4.9 (4.2–5.4)	4.6 (4.2–4.9)	= 0.3751	4.6 (4.2–5.1)	3.6 (3.3–3.7)	< 0.0001*	4.4 (4.1–4.7)	4.4 (3.9–5.1)	= 0.6001	4.6 (4.3–4.8)	2.9 (2.6–3.5)	< 0.0001*
Septal <i>a'</i> (cm/s)	5.3 (5.2–5.3)	3.6 (3.1–5.6)	= 0.2736	6.3 (5.0–6.7)	4.0 (3.6–4.8)	< 0.0001*	4.7 (4.5–5.0)	4.5 (3.6–5.3)	= 0.2441	4.4 (4.0–7.3)	3.6 (3.1–3.9)	< 0.0001*
E/Septal <i>e'</i>	24.3 (22.4–28.5)	24.3 (24.0–25.5)	= 0.7669	24.4 (22.2–29.5)	21.9 (20.1–22.7)	= 0.0397*	26.6 (25.6–28.7)	19.2 (16.0–23.4)	< 0.0001*	25.7 (23.0–28.6)	24.6 (20.5–28.0)	= 0.5056
Posterior <i>s'</i> (cm/s)	5.5 (4.4–8.5)	4.8 (4.5–4.9)	= 0.1956	6.0 (5.7–6.3)	3.7 (3.3–3.9)	< 0.0001*	4.5 (4.4–4.7)	5.3 (4.4–5.8)	= 0.0555	5.5 (5.3–6.2)	3.3 (3.0–3.8)	< 0.0001*
Posterior <i>e'</i> (cm/s)	6.0 (5.7–6.4)	5.7 (3.9–5.8)	= 0.0007*	7.3 (7.0–7.5)	4.2 (3.6–5.5)	< 0.0001*	4.9 (4.5–5.7)	4.6 (4.1–4.9)	= 0.1017	6.9 (6.6–7.0)	4.3 (3.5–4.7)	< 0.0001*
Posterior <i>a'</i> (cm/s)	5.0 (4.7–5.3)	5.7 (5.5–6.1)	< 0.0001*	7.1 (6.4–7.5)	5.0 (4.6–5.1)	< 0.0001*	5.7 (5.4–6.0)	5.3 (5.1–6.5)	= 0.7040	5.0 (4.0–6.3)	3.9 (3.0–4.5)	= 0.0008*
E/ Posterior <i>e'</i>	19.6 (18.8–21.2)	21.7 (19.0–28.3)	= 0.0540	15.5 (14.9–18.1)	18.3 (14.6–22.0)	= 0.0658	23.7 (21.1–26.8)	18.1 (17.4–21.0)	= 0.0026*	17.1 (16.1–18.2)	17.2 (13.7–21.4)	> 0.9999
LV length (mm)	10.6 (10.4–10.8)	11.1 (10.6–11.1)	= 0.0532	9.4 (9.1–11.3)	9.0 (9.0–10.5)	= 0.2020	9.9 (9.0–11.2)	11.7 (11.0–12.2)	< 0.0001*	10.0 (9.6–10.7)	9.0 (8.2–9.3)	< 0.0001*
IVRT (ms)	21 (20–23)	20 (15–23)	= 0.2321	20 (20–23)	29 (27–29)	< 0.0001*	21 (19–23)	24 (24–27)	< 0.0001*	21 (20–21)	43 (40–48)	< 0.0001*
RVOT pV (cm/s)	94 (86–99)	101 (90–102)	= 0.2285	95 (86–103)	76 (61–81)	= 0.0001*	87 (78–107)	77 (73–85)	= 0.0338*	95 (87–107)	64 (60–66)	< 0.0001*
LVOT pV (cm/s)	117 (114–123)	113 (109–117)	= 0.0302*	123 (112–149)	80 (76–82)	< 0.0001*	119 (112–127)	112 (92–119)	= 0.0257*	117 (114–126)	61 (55–65)	< 0.0001*
PEP (ms)	25 (25–28)	24 (24–27)	= 0.2542	24 (21–27)	32 (24–35)	= 0.0002*	27 (24–28)	28 (24–29)	= 0.9999	24 (21–27)	33 (32–37)	< 0.0001*
ET (ms)	85 (78–98)	81 (78–86)	= 0.3713	90 (80–96)	100 (78–105)	= 0.1374	92 (82–101)	77 (74–84)	= 0.0024*	88 (78–92)	113 (112–126)	< 0.0001*
Total IVPG	2.57 (2.40–2.72)	2.30 (2.28–2.72)	= 0.3397	2.52 (2.44–2.79)	1.96 (1.85–2.11)	< 0.0001*	2.48 (2.35–2.61)	2.13 (1.83–2.30)	< 0.0001*	2.21 (2.14–2.49)	1.36 (1.20–1.73)	< 0.0001*
Basal IVPG	1.62 (1.53–1.73)	1.51 (1.44–1.54)	= 0.0565	1.81 (1.65–1.91)	1.17 (1.07–1.33)	< 0.0001*	1.71 (1.60–1.87)	1.32 (1.18–1.60)	= 0.0031*	1.55 (1.47–1.75)	0.85 (0.68–1.08)	< 0.0001*
Mid IVPG	0.60 (0.54–0.69)	0.67 (0.64–0.70)	= 0.0867	0.58 (0.54–0.74)	0.65 (0.60–0.67)	= 0.2806	0.56 (0.44–0.66)	0.53 (0.45–0.61)	= 0.5874	0.57 (0.45–0.60)	0.44 (0.35–0.48)	= 0.0003*
Apical IVPG	0.20 (0.13–0.22)	0.14 (0.09–0.20)	= 0.0871	0.20 (0.16–0.24)	0.16 (0.12–0.21)	= 0.0489*	0.21 (0.15–0.26)	0.18 (0.16–0.26)	= 0.8941	0.20 (0.16–0.23)	0.11 (0.07–0.15)	< 0.0001*

**Table 1.** Continued

Parameters	CT			DM			CM			DMCM		
	PRE	POST	P	PRE	POST	P	PRE	POST	P	PRE	POST	P
Midapical	0.77	0.80	= 0.2797	0.77	0.78	= 0.9918	0.77	0.72	= 0.2287	0.72	0.55	< 0.0001*
IVPG	(0.74–0.82)	(0.75–0.84)		(0.69–0.89)	(0.75–0.85)		(0.70–0.82)	(0.62–0.79)		(0.68–0.82)	(0.42–0.58)	

BW body weight, BG blood glucose, LVIDd left ventricular internal diameter at diastole, LVIDs left ventricular internal diameter at systole, LVPWd left ventricular posterior wall at diastole, LVPWs left ventricular posterior wall at systole, LVM left ventricular mass, HR heart rate, E peak velocity of early diastole, A peak velocity of late diastole, *Septal s', e' and a'* tissue Doppler of systolic, early diastolic, and late diastolic wave velocities at septal mitral annulus, *Posterior s', e' and a'* tissue Doppler of systolic, early diastolic, and late diastolic wave velocities at posterior mitral annulus, LV length left ventricular length (measured from closed mitral valve (early systole) to apex in apical 4-chamber view), IVRT isovolumic relaxation time, RVOT right ventricular outflow tract, LVOT left ventricular outflow tract, PEP preejection period, ET ejection time, IVPG intraventricular pressure gradient (mm Hg/cm), CT control group, DM diabetic group, CM cardiomyopathic group, DMCM diabetic and cardiomyopathic group, FU fusion of E and A waves, PF partial fusion of E and A waves, SP separation of E and A waves. \*P < 0.05 PRE compared with POST

**Table 2.** The echocardiographic and other parameters after the induction of the diseases for 2 mo.

Parameters	CT	DM	CM	DMCM
BW (g)	329 (309–342)	300 (268–315)*	336 (316–352) <sup>f</sup>	253 (226–277) <sup>g,Δ</sup>
BG (mg/dL)	137 (111–161)	475 (442–501)*	107 (92–140) <sup>f</sup>	473 (422–502) <sup>g,Δ</sup>
LVIDd (mm)	8.0 (7.5–8.3)	7.4 (6.7–7.6)*	8.8 (8.5–9.1) <sup>f,Δ</sup>	7.8 (7.4–8.2) <sup>g</sup>
LVIDs (mm)	5.3 (4.8–5.4)	4.4 (4.3–4.8)	5.8 (5.5–6.1) <sup>f</sup>	4.9 (3.4–5.3) <sup>g</sup>
LVPWd (mm)	1.6 (1.6–1.8)	1.4 (1.2–1.6)	2.0 (1.9–2.1) <sup>f,Δ</sup>	1.4 (1.3–1.5) <sup>g</sup>
LVPWs (mm)	2.2 (2.2–2.4)	2.5 (2.0–2.5)	2.8 (2.7–2.9) <sup>f,Δ</sup>	2.8 (2.0–3.1)
LVM (mg)	757 (693–775)	518 (463–544)*	1075 (945–1117) <sup>f</sup>	640 (532–741) <sup>g</sup>
HR (bpm)	320 (293–323)	270 (251–275)*	290 (283–300)	222 (214–231) <sup>f,Δ,Δ</sup>
E (cm/s)	110 (107–120)	77 (74–82)*	89 (74–98) <sup>#</sup>	74 (59–76) <sup>f</sup>
Septal s' (cm/s)	3.5 (2.9–6.3)	2.9 (2.7–3.2)	3.6 (2.9–3.9)	2.1 (1.8–2.5) <sup>f,Δ,Δ</sup>
Septal e' (cm/s)	4.6 (4.2–4.9)	3.6 (3.3–3.7)*	4.4 (3.9–5.1) <sup>f</sup>	2.9 (2.6–3.5) <sup>f,Δ</sup>
Septal a' (cm/s)	3.6 (3.1–5.6)	4.0 (3.6–4.8)	4.5 (3.6–5.3)	3.6 (3.1–3.9) <sup>g</sup>
E/Septal e'	24.3 (24.0–25.5)	21.9 (20.1–22.7)	19.2 (16.0–23.4) <sup>#</sup>	24.6 (20.5–28.0)
Posterior s' (cm/s)	4.8 (4.5–4.9)	3.7 (3.3–3.9)*	5.3 (4.4–5.8) <sup>f</sup>	3.3 (3.0–3.8) <sup>f,Δ</sup>
Posterior e' (cm/s)	5.7 (3.9–5.8)	4.2 (3.6–5.5)	4.6 (4.1–4.9)	4.3 (3.5–4.7)
Posterior a' (cm/s)	5.7 (5.5–6.1)	5.0 (4.6–5.1)*	5.3 (5.1–6.5)	3.9 (3.0–4.5) <sup>f,Δ</sup>
E/Posterior e'	21.8 (19.0–28.3)	18.3 (14.6–22.0)	18.1 (17.4–21.0)	17.2 (13.7–21.4) <sup>f</sup>
LV length (mm)	11.0 (10.6–11.1)	9.0 (9.0–10.5)*	11.7 (11.0–12.2) <sup>f</sup>	9.0 (8.2–9.3) <sup>f,Δ</sup>
IVRT (ms)	20 (15–23)	29 (27–29)*	24 (24–27)	43 (40–48) <sup>f,Δ,Δ</sup>
RVOT pV (cm/s)	101 (90–102)	76 (61–81)*	77 (73–85) <sup>#</sup>	64 (60–66) <sup>g,Δ</sup>
LVOT pV (cm/s)	113 (109–117)	80 (76–82)*	112 (92–119) <sup>f</sup>	61 (55–65) <sup>g,Δ</sup>
PEP (ms)	24 (24–27)	32 (24–35)*	28 (24–29)	33 (32–37) <sup>g,Δ</sup>
ET (ms)	81 (78–86)	100 (78–105)	77 (74–84) <sup>f</sup>	113 (112–126) <sup>f,Δ,Δ</sup>
Total IVPG	2.30 (2.28–2.72)	1.96 (1.85–2.11)*	2.12 (1.83–2.30)	1.36 (1.20–1.73) <sup>f,Δ,Δ</sup>
Basal IVPG	1.51 (1.44–1.54)	1.17 (1.07–1.33)*	1.32 (1.18–1.60)	0.85 (0.68–1.08) <sup>f,Δ</sup>
Mid IVPG	0.67 (0.64–0.70)	0.65 (0.60–0.67)	0.53 (0.45–0.61) <sup>#</sup>	0.44 (0.35–0.48) <sup>f,Δ</sup>
Apical IVPG	0.14 (0.09–0.20)	0.16 (0.12–0.21)	0.18 (0.16–0.26)	0.11 (0.07–0.15) <sup>g</sup>
Midapical IVPG	0.80 (0.75–0.84)	0.78 (0.75–0.85)	0.72 (0.62–0.79)	0.55 (0.42–0.58) <sup>f,Δ,Δ</sup>

LVIDd left ventricular internal diameter at diastole, LVIDs left ventricular internal diameter at systole, LVPWd left ventricular posterior wall at diastole, LVPWs left ventricular posterior wall at systole, LVM left ventricular mass, RWT relative wall thickness, HR heart rate, E peak velocity of early diastole, *Septal s', e' and a'* tissue Doppler of systolic, early diastolic, and late diastolic wave velocities at septal mitral annulus, *Posterior s', e' and a'* tissue Doppler of systolic, early diastolic, and late diastolic wave velocities at posterior mitral annulus, LV length left ventricular length (measured from closed mitral valve (early systole) to apex in apical 4-chamber view), IVRT isovolumic relaxation time, RVOT right ventricular outflow tract, LVOT left ventricular outflow tract, PEP preejection period, ET ejection time, IVPG intraventricular pressure gradient (mm Hg/cm), CT control group, DM diabetic group, CM cardiomyopathic group, DMCM diabetic, and cardiomyopathic group

\*P < 0.05 CT compared with DM

<sup>#</sup>P < 0.05 CT compared with CM

<sup>f</sup>P < 0.05 CT compared with DMCM

<sup>Δ</sup>P < 0.05 DM compared with CM

<sup>Δ,Δ</sup>P < 0.05 DM compared with DMCM

<sup>g,Δ,Δ</sup>P < 0.05 CM compared with DMCM

and isoproterenol as described for the induction of both DM and cardiomyopathy in individual rats. The CT group (n = 15) underwent single intraperitoneal injection of 0.9% normal

saline. Both streptozotocin and isoproterenol were available as powders, and were dissolved with 0.9% normal saline in sterile technique before injection. Solutions were used within 30 min

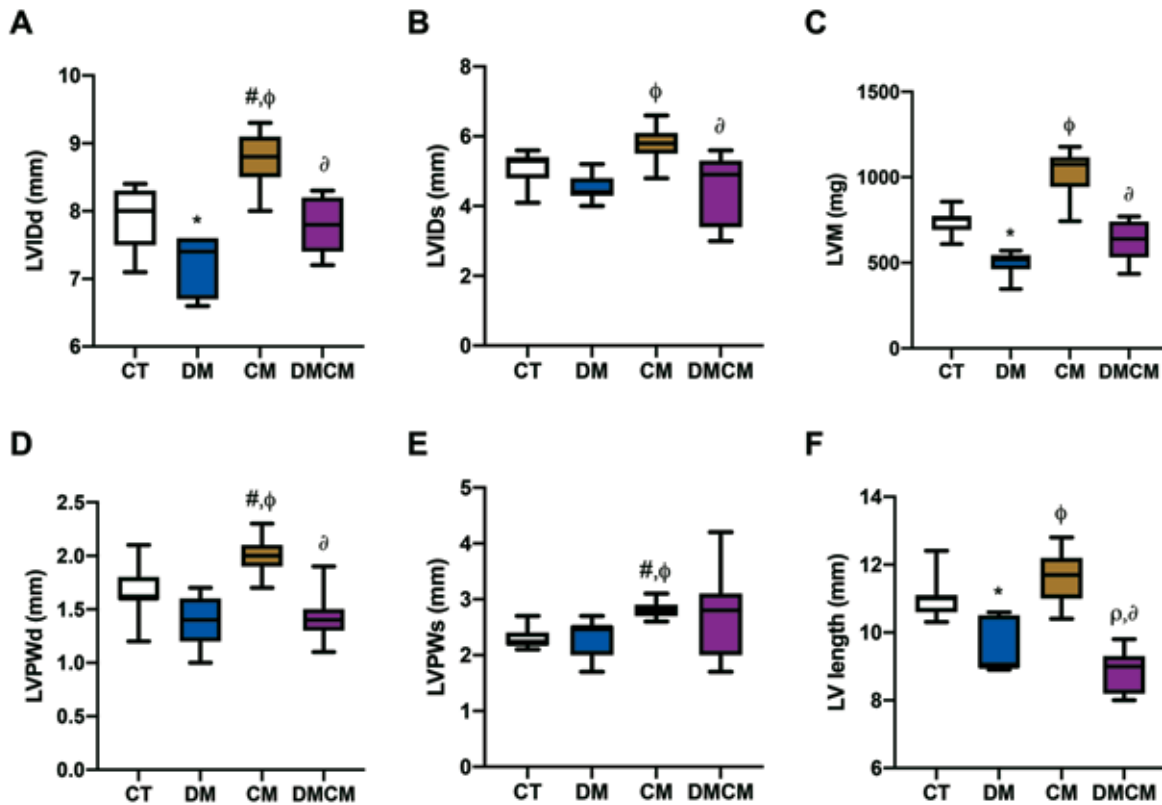


**Figure 2.** Ventricular dimension and mass indices with (A) *LVIDd* left ventricular internal diameter at end diastole, (B) *LVIDs* left ventricular internal diameter at systole, (C) *LVM* left ventricular mass, (D) *LVPWd* left ventricular posterior wall thickness at end diastole, (E) *LVPWs* left ventricular posterior wall at systole, and (F) *LV length* left ventricular length (measured from closed mitral valve (early systole) to apex in apical 4-chamber view). *CT* control group, *DM* diabetic group, cardiomyopathy cardiomyopathic group, *DMCM* diabetic, and cardiomyopathic group. \**P* < 0.05 *CT* compared with *DM*, #*P* < 0.05 *CT* compared with *CM*, ϕ*P* < 0.05 *CT* compared with *DMCM*, ∂*P* < 0.05 *DM* compared with *CM*, ρ*P* < 0.05 *DM* compared with *DMCM*, ∂*P* < 0.05 *CM* compared with *DMCM*

and maintained at 4 °C because they were highly degradable.<sup>19</sup> All procedures and protocols used in this experiment were approved at the Tokyo University of Agriculture and Technology and were performed consistent with guidelines described in the *Guide for the Care and Use of Laboratory Animals*.<sup>12</sup>

**Echocardiographic measurements.** Echocardiography was performed on all subjects before and at 2 mo after induction of DM and/or CM. Isoflurane was used for anesthesia because of its minimal effect on heart rate (HR) and its smooth recovery.<sup>11</sup> Spontaneous breathing was used during anesthesia induction and maintenance. Mask inhalation of 5% isoflurane, with 2.5 L/min oxygen, was used for induction; then the isoflurane was reduced to 2.5% for maintenance. Each echocardiographic analysis took about 30 min. The rats were shaved over the chest area, positioned laterally, and instrumented with ECG leads. The right parasternal short axis at papillary muscle level and the aorta-main pulmonary artery level were obtained with the rat in right lateral recumbency. Then the rat was positioned in left lateral recumbency for obtaining the left parasternal long axis apical four and five chambers views. The alligator ECG leads were clipped to the rat's paws at both forelimbs and the left hindlimb. An echocardiography machine (Aloka Medical ProSound Premier CV, Hitachi, Tokyo, Japan) with a 12-MHz probe was used according to the American Society of Echocardiography guidelines.<sup>24</sup> Conventional echocardiography, Doppler ultrasonography of blood flow and tissue, diastolic color Doppler M-mode imaging, and 2DTT were recorded 5 consecutive times and then averaged. Early (E) and late (A) mitral inflow was categorized into complete fusion,

partial fusion, and complete separation. As a measure of heart size, the LV mass (*LVM*) index was calculated according to the following equation:<sup>18</sup>

$$\text{LV mass (mg)} = 1.04 \times \left( \left[ \text{LVIDd} + \text{LVPWd} + \text{IVSd} \right]^3 - \text{LVIDd}^3 \right) \times 0.8 + 0.14.$$

Myocardial velocities were obtained by using pulsed-wave tissue Doppler imaging. The systolic (*s'*) and diastolic (*e'* and *a'*) myocardial velocities of the annuli descending toward the apex in systole and ascending away from the apex in diastole were measured from both septal and posterior regions. The diastolic color Doppler M-mode images were captured, saved, and then analyzed by using the MATLAB software (MatWorks version 9.1.0.441655 [R2016b]) with a specific equation for IVPG analysis,

$$\frac{\partial p}{\partial s} = -p \left[ \frac{\partial v}{\partial t} + v \frac{\partial v}{\partial s} \right].$$

In this equation, *p*, blood density, *p*, local pressure, *v*, velocity, *s*, space and *t*, is time, respectively. Figure 1 describes the process of analyzing intraventricular pressure difference (IVPD). The apical 4-chamber view was acquired by using a rate of 70 to 110 frames per second, saved onto a hard drive, and then analyzed offline (DAS-RS1 version 6.0, Hitachi) for 2DTT evaluation.

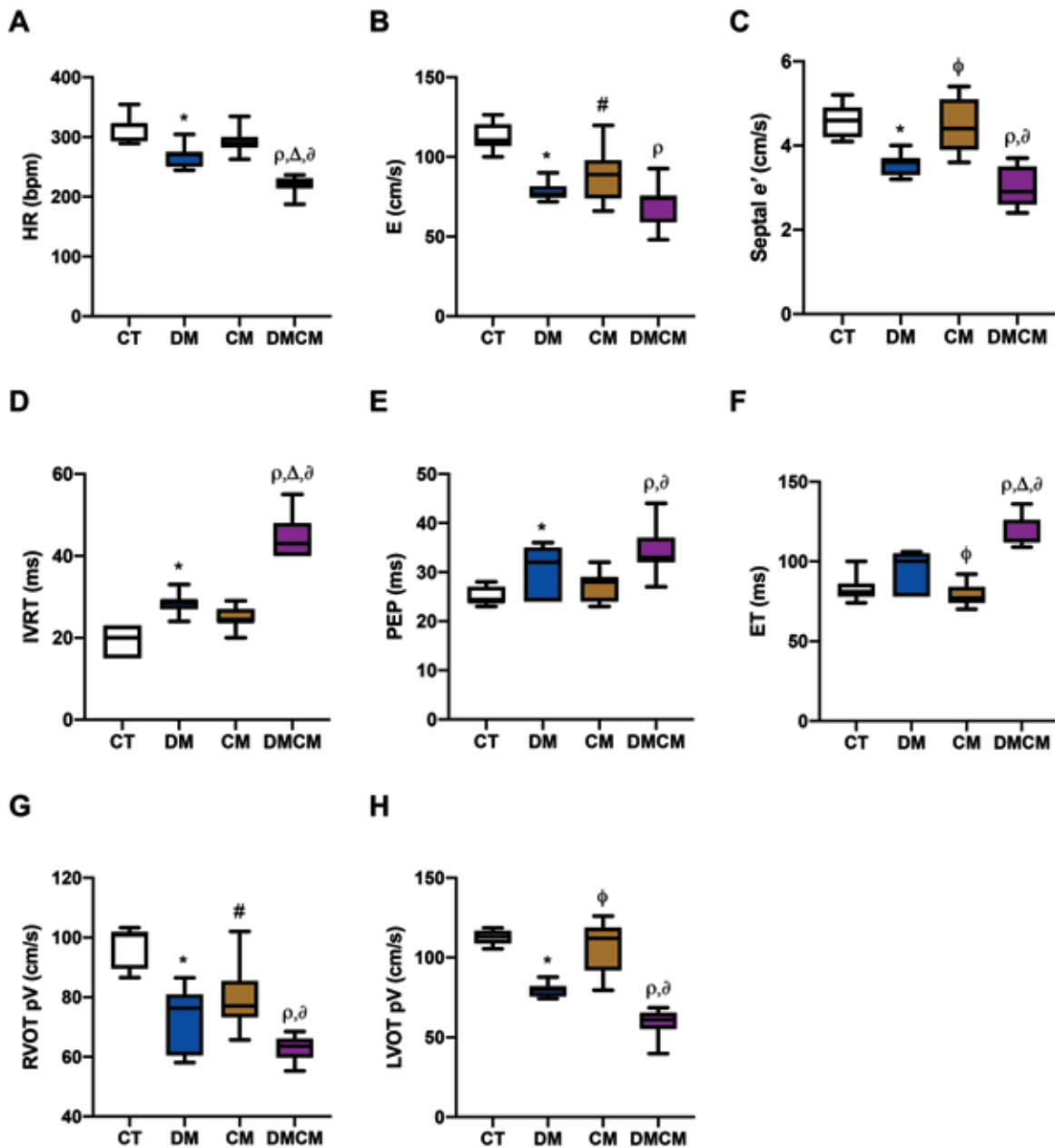


**Figure 3.** Ventricular performance indices with (A) HR heart rate, (B) E mitral inflow at early diastole, (C) Septal e' tissue Doppler of septal mitral annulus at early diastole, (D) IVRT isovolumic relaxation time, (E) PEP pre-ejection period, (F) ET ejection time, (G) RVOT pV peak velocity of right ventricular outflow tract, and (H) LVOT pV peak velocity of left ventricular outflow tract. CT control group, DM diabetic group, CM cardiomyopathic group, DMCM diabetic and cardiomyopathic group. \**P* < 0.05 CT compared with DM, #*P* < 0.05 CT compared with CM, <sup>ρ</sup>*P* < 0.05 CT compared with DMCM, <sup>Δ</sup>*P* < 0.05 DM compared with CM, <sup>∂</sup>*P* < 0.05 DM compared with DMCM, <sup>φ</sup>*P* < 0.05 CM compared with DMCM

**Histopathologic evaluation.** Two months after disease induction, all rats were euthanized by using isoflurane overdose. After euthanasia, the heart was immediately removed and rinsed with the normal saline. Formalin was used to preserve the tissue, which was processed using the standard paraffin-embedding technique. Masson trichrome (MTC) staining was used to assess tissue fibrosis in a blind evaluation by 2 pathologists, who examined 5 slides for each group. Cardiac fibrosis was evaluated by grading MTC positivity: grade 0, no MTC-positive regions; 1, mild or localized MTC staining; 2, moderate or multifocal MTC staining; and 3, extensive or diffuse, patchy MTC staining.

**Statistical analysis.** Nonparametric statistical analysis was used in this study due to the lack of normality of some data, as tested by using the Kolmogorov–Smirnov normality test. All data were expressed as the median with 25th to 75th percentiles. Mann–Whitney testing was used to compare results before and after disease induction in each group, and Kruskal–Wallis testing with the Dunn multiple-comparisons test was used to compare the results after disease induction among the 4 groups. All statistical analyses were performed by using the commercial software package Prism 7.0a for Macintosh (GraphPad Software, La Jolla, CA). A *P* value less than 0.05 was used to define significance.

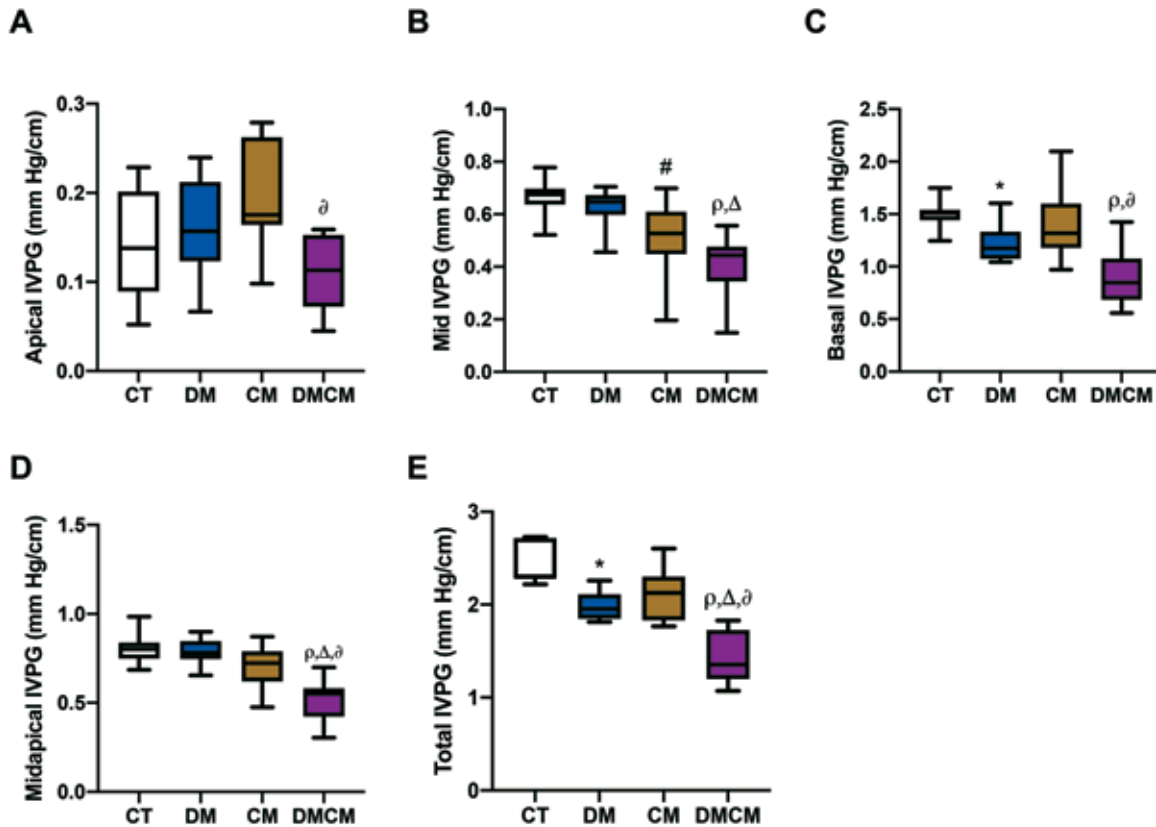


**Figure 4.** Intraventricular pressure gradient (IVPG) is divided into 3 different parts which are (A) apical, (B) middle, and (C) basal IVPGs. The grouping of middle and apical IVPGs into (D) midapical IVPG, and the grouping of all IVPGs into (E) total IVPG. CT control group, DM diabetic group, CM cardiomyopathic group, DMCM diabetic and cardiomyopathic group. \* $P < 0.05$  CT compared with DM, # $P < 0.05$  CT compared with CM,  $\Delta$  $P < 0.05$  CT compared with DMCM,  $\rho$  $P < 0.05$  DM compared with DMCM,  $\delta$  $P < 0.05$  CM compared with DMCM

## Results

Table 1 presents values for body weight, blood glucose, conventional echocardiographic parameters, and IVPG parameters before enrollment to the experiment and at 2 mo after the induction of DM and CM. Table 2 compares the associated parameters among the 4 groups at 2 mo after disease induction. LV internal dimensions (inner diameter and length) were significantly higher ( $P < 0.05$ ) in the CM group (5.8 to 8.8 mm and 11.7 mm) but lower ( $P < 0.05$ ) in the DM group (4.4 to 7.4 mm and 9.0 mm) (Figure 2 A, B, and F) compared to CT group. Similarly, LV posterior wall thickness was higher in the CM group as compared with both control rats and the DM group (Figure 2 D and E). The mass index of the heart (LVM) was greater in the CM group (1075 mg) than in the DM and DMCM groups. After disease was induced, the LVM was significantly higher ( $P < 0.05$ ) in the CM group as compared with the DM group but significantly lower ( $P < 0.05$ ) in the DM group as compared with the CT group (Figure 2 C). LVM is used to indicate the mass index of LV.

HR in diabetic groups (DM and DMCM groups) was lower, especially in the DMCM group (Figure 3 A) than in the CT group. All treatment groups showed significantly decreased ( $P < 0.05$ ) E waves (from 74 to 89 cm/s) after developing disease (Figure 3 B). The patterns of the E and A waves differed among the groups (Table 1). Tissue Doppler imaging parameters, including septal and posterior  $s'$ ,  $e'$ , and  $a'$ , from the single-disease groups were not different from the control group. In contrast, almost all of these parameters, except for posterior  $e'$  and septal  $a'$ , differed ( $P < 0.05$ ) between DMCM and control rats. A

significant decrease in E/septal  $e'$  occurred only the CM group, and a significant decrease ( $P < 0.05$ ) of E/posterior  $e'$  was found only in the DMCM group (Table 2). Moreover, isovolumic relaxation time, preejection period, and ejection time (IVRT, PEP, and ET, respectively) were prolonged in the disease groups, particularly in the DMCM group (Figure 3 D through F), and the peak right and left ventricular outflow velocities were decreased in all treatment groups, especially in the DMCM group (Figure 3 G and H). The E wave, septal  $e'$ , and right and left ventricular outflow tracks had similar patterns, which were lower in the DM and DMCM groups and higher in the CM group as compared with the CT group (Figure 3 B, C, G and H). The combination of 2 conditions (DMCM group) led to the most severe decrease, with the decreases in these parameters in the DM group falling between those of the DMCM and CM groups.

IVPG are divided into 3 segments: basal, middle, and apical IVPG. Apical IVPG was lower in the DMCM group but higher in the CM and DMCM groups as compared with CT group (Figure 4 A). The apical IVPG of the DMCM group was significantly lower than the CM group. The middle-segment IVPG was lower in the CM and DMCM groups than in the controls and in the DMCM group as compared with the DM group. Combining the apical and middle segments revealed that the DMCM group was significantly lower than the other groups. Diabetic rats (the DM and DMCM groups) showed a significant decrease of basal IVPG ( $P < 0.05$ ) as compared with the controls (Figure 4 C). For these reasons, the total IVPG of the DMCM group was lower than that of all other groups, and that of the DM group

**Table 3.** The values of each strain in 2-dimensional tissue tracking (2DTT).

Strains	Strain				Speed			
	CT	DM	CM	DMCM	CT	DM	CM	DMCM
<b>Begin Time</b>								
D	252 (244–260)	272 (254–295)	279 (274–284)	362 (301–376) <sup>r</sup>	252 (244–260)	272 (254–295)	279 (274–284)	362 (301–376) <sup>r</sup>
E	252 (242–260)	285 (270–307)*	274 (266–284)	362 (319–370) <sup>r</sup>	252 (242–260)	285 (270–307)*	274 (266–284)	362 (319–370) <sup>r</sup>
F	252 (252–260)	297 (264–309)*	274 (274–284)	366 (344–372) <sup>r</sup>	252 (252–260)	297 (264–309)*	274 (274–284)	366 (344–372) <sup>r</sup>
G	252 (244–253)	289 (270–315)*	279 (274–284)	370 (344–390) <sup>r</sup>	252 (244–253)	289 (270–315)*	279 (274–284)	370 (344–390) <sup>r</sup>
H	244 (244–252)	289 (262–309)	279 (274–284)	370 (342–382) <sup>r</sup>	244 (244–252)	289 (262–309)	279 (274–284)	370 (342–382) <sup>r</sup>
J	244 (244–252)	289 (260–309)	279 (266–292)	378 (360–392) <sup>r</sup>	244 (244–252)	289 (260–309)	279 (266–292)	378 (360–392) <sup>r</sup>
K	244 (236–252)	285 (260–309)	284 (274–292)	347 (260–368) <sup>r</sup>	244 (236–252)	260 (260–309)	284 (274–292) <sup>#</sup>	347 (260–368) <sup>r</sup>
<b>Peak Time</b>								
D	326 (317–333)	370 (342–398)	368 (368–387)	464 (429–482) <sup>r</sup>	277 (277–285)	321 (289–350)	316 (305–326)	419 (396–437) <sup>r</sup>
E	326 (317–333)	370 (335–403)	368 (368–387)	468 (429–488) <sup>r</sup>	277 (277–285)	333 (289–350)	316 (308–332)	423 (390–437) <sup>r</sup>
F	326 (317–333)	370 (344–390)	368 (368–387) <sup>#</sup>	472 (429–490) <sup>r</sup>	277 (277–284)	329 (289–348)	316 (316–326)	423 (396–429) <sup>r</sup>
G	326 (317–333)	370 (342–417)	368 (368–387)	472 (429–490) <sup>r</sup>	277 (268–285)	325 (289–366)	311 (305–316)	419 (401–429) <sup>r</sup>
H	326 (317–333)	370 (342–417)	368 (368–387) <sup>#</sup>	476 (429–490) <sup>r</sup>	277 (268–285)	329 (295–348)*	311 (297–324)	415 (394–425) <sup>r</sup>
J	317 (309–333)	370 (344–411)	368 (368–387)	472 (429–490) <sup>r</sup>	274 (268–277)	325 (287–342)*	305 (305–313)	407 (388–419) <sup>r,†</sup>
K	309 (300–333)	362 (344–396)	368 (368–387) <sup>#</sup>	451 (409–488) <sup>r</sup>	268 (263–277)	313 (285–342)*	300 (295–313) <sup>#</sup>	403 (364–417) <sup>r</sup>

CT control group, DM diabetic group, CM cardiomyopathic group, DMCM diabetic and cardiomyopathic group

D, E, F, G, H, J, and K are strains (Figure 5 A)

\* $P < 0.05$  CT compared with DM

<sup>#</sup> $P < 0.05$  CT compared with CM

<sup>r</sup> $P < 0.05$  CT compared with DMCM

<sup>†</sup> $P < 0.05$  CM compared with DMCM

was lower than the controls. However, the total IVPG of the CM group was normal, with the middle segment significantly lower ( $P < 0.05$ ) than the control group.

The 2DTT results are shown in Table 3. The A, B, and C strains of the 2DTT represent the basal segment of the LV; the D, E, F, and G strains indicate the middle segment of the LV; and the H, J, and K strains represented the apical segment of the LV (Figure 5 A). In this experiment, the middle and apical segments (D, E, F, G, H, J, and K strains) were used for interpretation. These data represented the values during the LV diastole, tracking the wall movement at the relaxation period. Both the baseline and peak times were delayed in all treatment groups as compared with CT group, and the DMCM group showed the most prolonged pause ( $P < 0.05$ ) among the 3 treatment groups (Figure 5). Although some strains of the middle segment differed significantly between the DM and CM groups, only the DMCM group differed significantly from the control group.

The degree of fibrosis was evaluated at 2 mo after disease induction (Figure 6). The DMCM group had the most fibrotic tissue, which showed diffuse accumulation of positive MTC (grade 3) staining in many areas, especially in subendocardial area. In addition, moderate fibrosis (grade 2) was present in the CM group, also notably in the subendocardial area. In the DM group, subtle fibrotic areas (grade 1) were identified in specific areas, including perivascular and some interstitial tissues. Controls showed no MTC-positive areas (grade 0).

## Discussion

Compared with the control group, LV dimension and mass parameters were lower in the DM groups but higher in the CM group. Furthermore, the heart was smaller in the DM groups, as shown by its lower LV length and LVM as compared with the CM group. In contrast, LV wall thickness and other dimension parameters of the CM group were highest among all groups. For these reasons, the decrease of the LVM and LV length of the

DM group led to the relative increase in those parameters in the CM group when compared with the CT group. The DM and CM groups showed different patterns of dimensional change. In the DM rats, both the LVM and the body weight were decreased as compared with the CT group. A previous study demonstrated that streptozotocin causes insulin deficiency and uncontrolled diabetes leading to muscle atrophy and decreased muscle strength.<sup>20</sup> The decrease of ventricular geometry parameters in the DM group resulted in the smallest size of the heart among groups. Our previous study also showed that the DM rats had a significant loss of body weight after developing DM.<sup>14</sup> In comparison to DM group, the CM group showed a significant increase in LVM and LV length; the cardiac modifications associated with isoproterenol-induced cardiomyopathy include hypertrophy, dilation, and ventricular dysfunction.<sup>4</sup> Therefore, these parameters were within control limits in the DMCM group because the alterations due to DM and CM were opposite to each other. The increases in ventricular dimension and mass were supported by the accumulated fibrotic tissue of the isoproterenol-induced CM group. Given that ISO causes myocardial infarction and subsequent fibrosis formation during the repair process, myocardial fibrosis is important in the remodeling of the heart.<sup>10,28</sup>

Prolonged hyperglycemia results in the enhanced generation of advanced glycated end products, increased glucose auto-oxidation, and oxidative phosphorylation, leading to oxidative stress.<sup>7</sup> Hyperglycemia causes the formation of reactive oxygen species, which are important contributors to the adverse effects of DM. The primary source of reactive oxygen species is the respiratory chain of mitochondria. During persistent hyperglycemia, mitochondria produce  $O_2^-$  in cells, leading to mitochondrial dysfunction.<sup>25</sup> The chronic oxidative stress under hyperglycemic conditions leads to mutation or transformation of DNA, resulting in cell death due to necrosis or apoptosis.<sup>8,26</sup> An increase in myocardial apoptosis is a necessary consequence of the development of diabetic cardiomyopathy. Compared



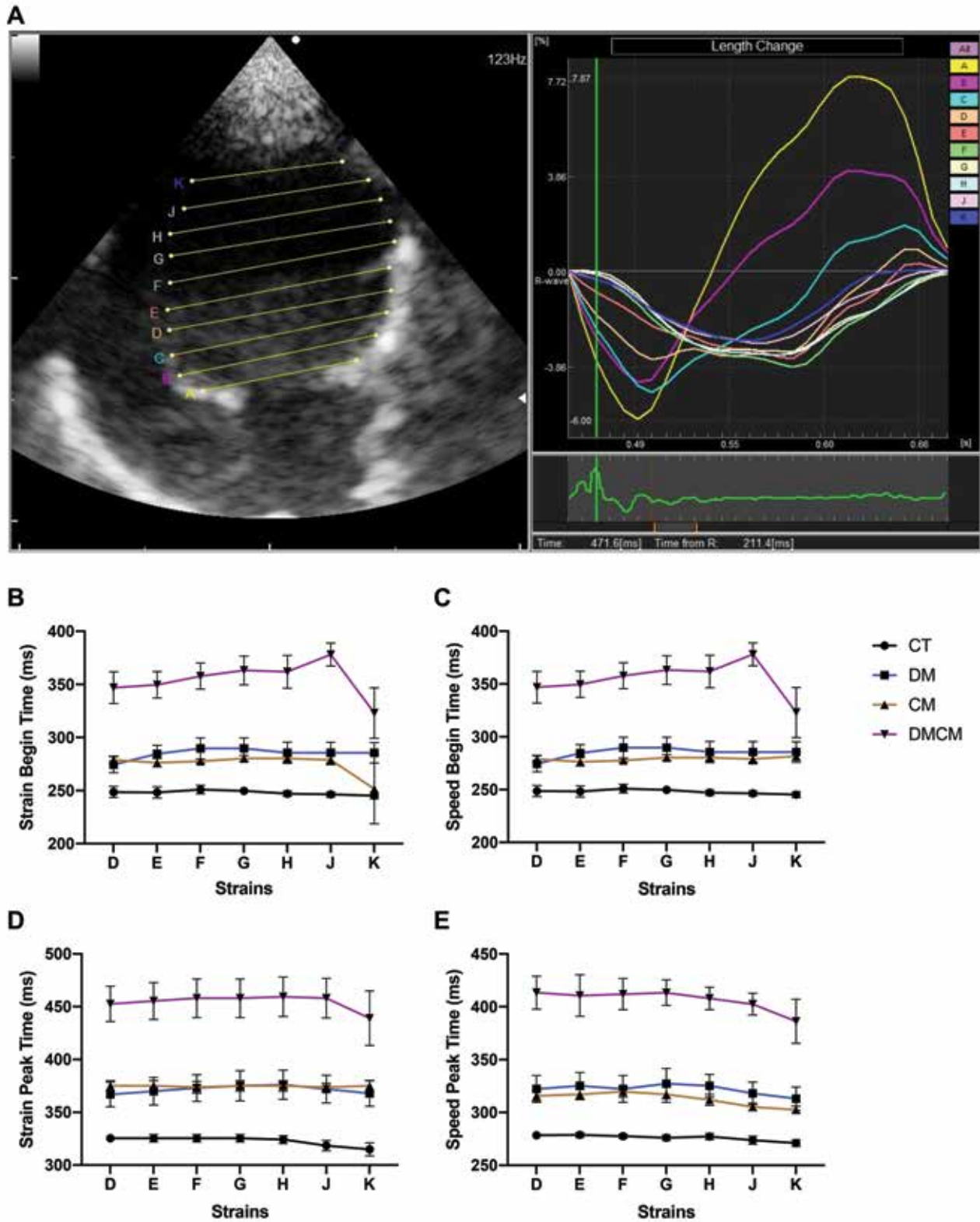
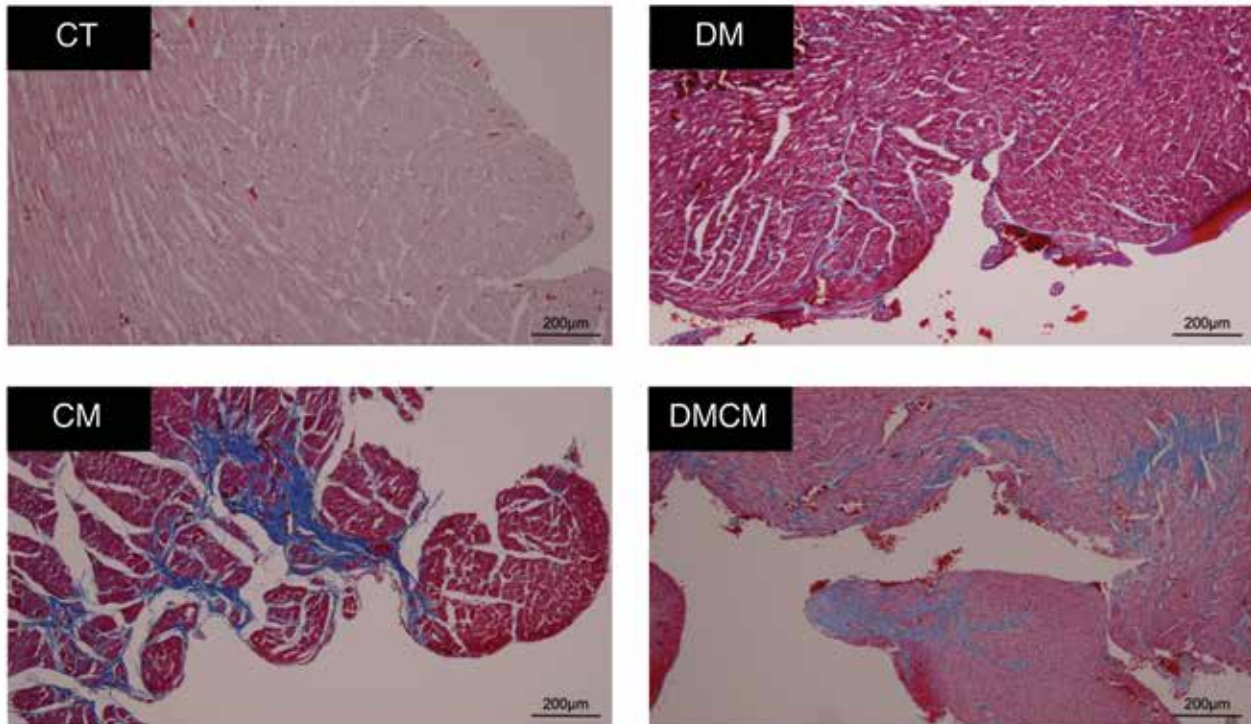


Figure 5. (A) 2D tissue tracking (2DTT) is analyzed by using the DAS-RS1 software 6.0v (Aloka). Each strain (A, B, C, D, E, F, G, H, J, and K) is drawn horizontally to the mitral valve for tracking the ability of relaxation (diastolic performance) of the LV. The 2DTT results are illustrated separately at begin (B and C) and peak (D and E) times. CT control group, DM diabetic group, CM cardiomyopathic group, DMCM diabetic and cardiomyopathic group.

with nondiabetic individuals, diabetic subjects had an 85-fold increase in the apoptosis of cardiomyocytes.<sup>22</sup> Impaired cardiac relaxation can result from metabolic dysfunction, such as impaired glucose uptake and utilization, accumulation of fuel

stores, and a shift toward fatty acid oxidation in the myocardium. Consequently, oxidative stress and autophagy lead to decreases in cardiac compliance (by causing fibrosis) and activation of cell death pathways. In other words, treatment with



**Figure 6.** The Masson trichrome (MTC) staining of the left ventricle. Positive areas represent in blue. Grading system of MTC positive: Grade 0; no positive area to Masson trichrome (no visible blue area). Grade 1; slightly positive area to Masson trichrome in interstitial or perivascular area. Grade 2; patchy or local positive area to Masson trichrome in interstitial, perivascular, and subendocardial areas. Grade 3; multifocal generalized positive area to Masson trichrome in many tissues of the heart. *CT* control group, *DM* diabetic group, *CM* cardiomyopathic group, *DMCM*, diabetic and cardiomyopathic group.

streptozotocin exacerbates diabetes-induced heart disease.<sup>27</sup> A previous publication showed that the myocardial phosphocreatinine–ATP index is reduced and associated with altered diastolic function in diabetic subjects.<sup>5</sup>

Cardiac work can be evaluated in many ways. The ‘gold standard’ uses LV catheterization to assess cardiac LV pressure–volume loops, but this method is invasive and is not practical for clinical routines. Instead, new advanced techniques of echocardiography have been developed. Diastole is divided into 4 distinct phases, which are isovolumic relaxation, early diastole (rapid filling), diastasis (slow filling), and atrial systole (final filling). Mitral inflow is divided mainly into early (E wave) and late (A wave) phases. The variation in the patterns of the E and A waves that we reported here were related to the HR. At slow heart rates (i.e., lower than 300 bpm), such as in humans, the period of time necessary for the heart to relax is long enough for the blood to fill the chambers in 2 distinct phases, early (E) and late (A) diastole. Therefore, E and A waves are usually seen in slow HR. In contrast, E and A waves are usually fused during fast HR. In the current experiment, isoflurane was chosen as an anesthetic because it has minimal effects on the heart, and healthy rats have high HR. Anesthesia of rats with heart disease led to the separation of E and A waves, as in the DMCM group, because of the lower HR. Therefore, HR and anesthesia protocols interact to change mitral inflow patterns.

Many echocardiographic parameters can be used to assess diastolic function. Our current study showed that diastolic dysfunction occurred in all treatment groups and was most severe in the DMCM rats. Several conventional parameters, such as mitral Doppler inflow during early diastole (E) and other Doppler parameters, especially septal and posterior  $e'$  and  $a'$ ,

can be used to assess diastolic functions. These measures decreased (Figure 3 B and C) in all treatment groups, indicating abnormal relaxation of the heart during diastole because of decreased compliance of the myocardium. The severe fibrosis in the DMCM group led to pronounced impairment of diastolic function, such as decreased E and septal  $e'$ . As diastolic dysfunction worsens, decreased compliance coexists with systolic abnormalities, including decreased peak outflow velocities of the right and left ventricles and a prolonged preejection period.

Conventional echocardiography and diastolic IVPG and 2DTT can all be used to assess diastolic function. In our current study, diabetic rats (i.e., the DM and DMCM groups) demonstrated a decrease of IVPGs (Figure 4) as compared with CT group. The overall IVPG of the CM group did not change significantly, but the middle IVPG segment decreased. As mentioned previously, cardiac fibrosis was prominent in the CM (grade 2) and DMCM (grade 3) groups and was the major cause of decreased compliance. The DM and DMCM groups showed prolongation of the isovolumic relaxation time, preejection period, and ejection time (Figure 3 D through F). Moreover, 2DTT confirmed that the prolonged relaxation time reflected the changes in the IVRT pattern. In 2DTT, both baseline and peak times lengthened significantly (Figure 5) in all treatment groups compared with controls. Among the treatment groups, the DMCM rats showed the most pronounced abnormalities, including prolonged 2DTT times, severe cardiac fibrosis, low HR, and abnormalities in all segments of IVPG.

In conclusion, diabetic cardiomyopathy and cardiomyopathy have different mechanisms of disease development. Conventional echocardiography cannot clearly distinguish between these similar diseases. Therefore, IVPG and 2DTT have been

developed and are widely used, as in this study, for obtaining precise information to confirm physiologic changes in the heart. By overcoming the limitations of conventional echocardiography, both IVPG and 2DTT can be used to assess cardiac performance that can be categorized into different heart segments such as apical, middle, or basal parts. Our current findings indicate that hyperglycemia, such as that of DM patients and when present with other cardiac conditions, is an important factor that can worsen cardiac performance. Moreover, IVPG and 2DTT are useful indices for assessing cardiac functions, especially for evaluating specific portions of the heart.

## References

- Albarrak AI, Mohammed R, Assery B, Allam D, Morit SA, Saleh RA, Zare'a R. 2018. Evaluation of diabetes care management in primary clinics based on the guidelines of American Diabetes Association. *Int J Health Sci (Qassim)* **12**:40–44.
- Asada-Kamiguchi J, Jones M, Greenberg NL, Popovic ZB, Tsujino H, Zetts AD, Qin JX, Garcia MJ, Thomas JD, Shiota T. 2006. Intraventricular pressure gradients in left ventricular aneurysms determined by color M-mode Doppler method: an animal study. *J Am Soc Echocardiogr* **19**:1112–1118. <https://doi.org/10.1016/j.echo.2006.04.015>.
- Athithan L, Gulsin GS, McCann GP, Levelt E. 2019. Diabetic cardiomyopathy: Pathophysiology, theories and evidence to date. *World J Diabetes* **10**:490–510. <https://doi.org/10.4239/wjd.v10.i10.490>.
- Chang SC, Ren S, Rau CD, Wang JJ. 2018. Isoproterenol-induced heart failure mouse model using osmotic pump implantation. *Methods Mol Biol* **1816**:207–220. [https://doi.org/10.1007/978-1-4939-8597-5\\_16](https://doi.org/10.1007/978-1-4939-8597-5_16).
- Diamant M, Lamb HJ, Groeneveld Y, Endert EL, Smit JW, Bax JJ, Romijn JA, de Roos A, Radder JK. 2003. Diastolic dysfunction is associated with altered myocardial metabolism in asymptomatic normotensive patients with well-controlled type 2 diabetes mellitus. *J Am Coll Cardiol* **42**:328–335. [https://doi.org/10.1016/S0735-1097\(03\)00625-9](https://doi.org/10.1016/S0735-1097(03)00625-9).
- Falsetti HL, Verani MS, Chen C-J, Cramer JA. 1980. Regional pressure differences in the left ventricle. *Cathet Cardiovasc Diagn* **6**:123–134. <https://doi.org/10.1002/ccd.1810060203>.
- Gauthier EL, editor. 2014. *Streptozotocin: uses, mechanism of action and side effects*. Hauppauge (NY): Nova Science Publishers.
- Ghfourifar P, Bringold U, Klein SD, Richter C. 2001. Mitochondrial nitric oxide synthase, oxidative stress and apoptosis. *Biol Signals Recept* **10**:57–65. <https://doi.org/10.1159/000046875>.
- Greenberg NL, Vandervoort PM, Firstenberg MS, Garcia MJ, Thomas JD. 2001. Estimation of diastolic intraventricular pressure gradients by Doppler M-mode echocardiography. *Am J Physiol Heart Circ Physiol* **280**:H2507–H2515. <https://doi.org/10.1152/ajpheart.2001.280.6.H2507>.
- Heather LC, Catchpole AF, Stuckey DJ, Cole MA, Carr CA, Clarke K. 2009. Isoproterenol induces in vivo functional and metabolic abnormalities: similar to those found in the infarcted rat heart. *J Physiol Pharmacol* **60**:31–39.
- Huss MK, Chum HH, Chang AG, Jampachairi K, Pacharinsak C. 2016. The physiologic effects of isoflurane, sevoflurane, and hypothermia used for anesthesia in neonatal rats (*Rattus norvegicus*). *J Am Assoc Lab Anim Sci* **55**:83–88.
- Institute for Laboratory Animal Research. 2011. *Guide for the care and use of laboratory animals*, 8th ed. Washington (DC): National Academies Press.
- Kimura K, Daimon M, Morita H, Kawata T, Nakao T, Okano T, Lee SL, Takenaka K, Nagai R, Yatomi Y, Komuro I. 2015. Evaluation of right ventricle by speckle tracking and conventional echocardiography in rats with right ventricular heart failure. *Int Heart J* **56**:349–353. <https://doi.org/10.1536/ihj.14-367>.
- Kitpipatkun P, Matsuura K, Shimada K, Uemura A, Goya S, Yoshida T, Ma D, Takahashi K, Tanaka R. 2020. Key factors of diastolic dysfunction and abnormal left ventricular relaxation in diabetic rats. *J Med Ultrason* **47**:347–356. <https://doi.org/10.1007/s10396-020-01021-x>.
- Li CJ, Chen CS, Yang GT, Tsai AP, Liao WT, Wu MY. 2019. Advanced evolution of pathogenesis concepts in cardiomyopathies. *J Clin Med* **8**:1–23.
- Ling D, Rankin JS, Edwards CH 2nd, McHale PA, Anderson RW. 1979. Regional diastolic mechanics of the left ventricle in the conscious dog. *Am J Physiol* **236**:H323–H330. <https://doi.org/10.1152/ajpheart.1979.236.2.H323>.
- Lobo Filho HG, Ferreira NL, Sousa RB, Carvalho ER, Lobo PL, Lobo Filho JG. 2011. Experimental model of myocardial infarction induced by isoproterenol in rats. *Rev Bras Cir Cardiovasc* **26**:469–476. <https://doi.org/10.5935/1678-9741.20110024>. [Article in En, Portuguese].
- Low Wang CC, Hess CN, Hiatt WR, Goldfine AB. 2016. Clinical update: cardiovascular disease in diabetes mellitus: Atherosclerotic cardiovascular disease and heart failure in type 2 diabetes mellitus—mechanisms, management, and clinical considerations. *Circulation* **133**:2459–2502. <https://doi.org/10.1161/CIRCULATIONAHA.116.022194>.
- Motyl K, McCabe LR. 2009. Streptozotocin, type I diabetes severity and bone. *Biol Proced Online* **11**:296–315. <https://doi.org/10.1007/s12575-009-9000-5>.
- O'Neill BT, Bhardwaj G, Penniman CM, Krumpoch MT, Suarez Beltran PA, Klaus K, Poro K, Li M, Pan H, Dreyfuss JM, Nair KS, Kahn CR. 2019. FoxO transcription factors are critical regulators of diabetes-related muscle atrophy. *Diabetes* **68**:556–570. <https://doi.org/10.2337/db18-0416>.
- Ono K, Masuyama T, Yamamoto K, Doi R, Sakata Y, Nishikawa N, Mano T, Kuzuya T, Takeda H, Hori M. 2002. Echo doppler assessment of left ventricular function in rats with hypertensive hypertrophy. *J Am Soc Echocardiogr* **15**:109–117. <https://doi.org/10.1067/mje.2002.115034>.
- Ouyang C, You J, Xie Z. 2014. The interplay between autophagy and apoptosis in the diabetic heart. *J Mol Cell Cardiol* **71**:71–80. <https://doi.org/10.1016/j.yjmcc.2013.10.014>.
- Poantã L, Fodor D, Albu A. 2010. Left ventricular function in patients with uncomplicated well-controlled diabetes mellitus. *Med Ultrason* **12**:184–187.
- Schiller NB, Shah PM, Crawford M, DeMaria A, Devereux R, Feigenbaum H, Gutgesell H, Reichek N, Sahn D, Schnittger I, Silverman NH, Tajik AJ. 1989. Recommendations for quantitation of the left ventricle by two-dimensional echocardiography. American Society of Echocardiography Committee on Standards, Subcommittee on Quantitation of Two-Dimensional Echocardiograms. *J Am Soc Echocardiogr* **2**:358–367. [https://doi.org/10.1016/S0894-7317\(89\)80014-8](https://doi.org/10.1016/S0894-7317(89)80014-8).
- Sifuentes-Franco S, Padilla-Tejeda DE, Carrillo-Ibarra S, Miranda-Díaz AG. 2018. Oxidative stress, apoptosis, and mitochondrial function in diabetic nephropathy. *Int J Endocrinol* **2018**:1–13. <https://doi.org/10.1155/2018/1875870>.
- Srinivasan S, Stevens M, Wiley JW. 2000. Diabetic peripheral neuropathy: evidence for apoptosis and associated mitochondrial dysfunction. *Diabetes* **49**:1932–1938. <https://doi.org/10.2337/diabetes.49.11.1932>.
- Varma U, Koutsifeli P, Benson VL, Mellor KM, Delbridge LMD. 2018. Molecular mechanisms of cardiac pathology in diabetes—experimental insights. *Biochim Biophys Acta Mol Basis Dis* **1864**:1949–1959. <https://doi.org/10.1016/j.bbdis.2017.10.035>.
- Wang QW, Yu XF, Xu HL, Zhao XZ, Sui DY. 2019. Ginsenoside re improves isoproterenol-induced myocardial fibrosis and heart failure in rats. *Evid Based Complement Alternat Med* **2019**:1–9.
- Yotti R, Bermejo J, Desco MM, Antoranz JC, Rojo-Alvarez JL, Cortina C, Allué C, Rodríguez-Abella H, Moreno M, García-Fernández MA. 2005. Doppler-derived ejection intraventricular pressure gradients provide a reliable assessment of left ventricular systolic chamber function. *Circulation* **112**:1771–1779. <https://doi.org/10.1161/CIRCULATIONAHA.104.485128>.